SCIENTIA AGROPECUARIA

Scientia Agropecuaria

Web page: http://revistas.unitru.edu.pe/index.php/scientiaagrop

Facultad de Ciencias Agropecuarias

Universidad Nacional de Trujillo

RESEARCH ARTICLE

Agroforestry and montane forest management as strategies to mitigate carbon loss and sustain ecosystem functions in the Central Andes of Peru

Karen I. Eckhardt[1, 2 *]; Alexander Gori Maia[3]; José André Noriega-Puglisevich[2]; Walescka Cachay Jara[2]

[1] Universidad Nacional Agraria La Molina, Lima, Perú.
[2] Grupo de Investigación REC (Restauración de Ecosistemas y Calidad Ambiental). Universidad Científica del Sur, Lima, Perú.
[3] Universidade Estadual de Campinas, São Paulo, Brasil.

* Corresponding author: keckhardt@lamolina.edu.pe (K. I. Eckhardt).

Received: 6 June 2025. Accepted: 5 October 2025. Published: 27 October 2025.

Abstract

Land-use change in the Central Andes of Peru has led to the widespread conversion of tropical montane forests, significantly reducing their carbon storage capacity. This study estimated aboveground and soil carbon stocks across a disturbance gradient: croplands (C), agroforestry systems (AF), regenerating montane forests (BMR), and conserved montane forests (BMC). Using destructive and non-destructive sampling, 61 plots (0.1 ha each) were assessed, measuring live and dead aboveground biomass, fine roots, and soil organic carbon down to 1 meter. Results show that BMC had the highest total carbon stock (575.33 ± 215.4 Mg C ha^{-1}), followed by BMR (386.53 ± 186.6), AF (276.69 ± 172.5), and C (205.14 ± 114.03). Soil organic carbon was the dominant carbon pool across all land uses, contributing between 93% (in croplands) and 62% (in conserved forests) of total carbon, highlighting its central role in carbon dynamics. Carbon stocks were significantly associated with vegetation structural attributes (basal area, diameter at breast height, canopy cover) and soil properties (texture, cation exchange capacity, organic matter content). Trees with diameter at breast height ≥ 30 cm contributed over 50% of aboveground carbon, underlining their importance in biomass carbon storage. These findings reveal a clear gradient of loss in the ecosystem service of carbon storage, driven by land-use intensification and the simplification of forest structure. However, they also demonstrate that the recovery of degraded forests and the implementation of agroforestry systems are viable strategies to reduce the loss of ecosystem functions and contribute meaningfully to climate change mitigation.

Keywords: carbon storage; soil organic carbon; tropical montane forest; agroforestry; land-use change; Central Andes.

DOI: https://doi.org/10.17268/sci.agropecu.2026.005

Cite this article:
Eckhardt, K. I., Maia, A. G., Noriega-Puglisevich, J. A., & Cachay Jara, W. (2026). Agroforestry and montane forest management as strategies to mitigate carbon loss and sustain ecosystem functions in the Central Andes of Peru. *Scientia Agropecuaria*, *17*(1), 77-89.

1. Introduction

Tropical montane forests are essential components for climate regulation, as their soils and biomass contribute significantly to carbon capture and storage, thereby helping to mitigate atmospheric concentrations of greenhouse gases such as carbon dioxide (CO_2) and methane (CH_4) (Díaz-Cháux et al., 2024). These ecosystems reveal much higher carbon stocks than previously estimated, particularly at higher elevations, up to 574 Mg ha^{-1} of aboveground biomass and 578 Mg ha^{-1} of soil carbon, suggesting that earlier lidar-based estimates may have substantially underestimated regional carbon reservoirs (Prada et al., 20025).

The conversion of tropical montane forests into agricultural land results in significant biodiversity loss and a pronounced decline in carbon storage capacity (Ojoatre et al., 2024). A recent synthesis of 63 studies indicates a mean decrease of ~12.6% in carbon stocks from 1975 to 2023, primarily due to deforestation for agriculture and forest degradation (Debie & Abro, 2025). Moreover, studies indicate that newly established forests often exhibit higher carbon sequestration efficiency than older, degraded ones, highlighting the importance of forest age in carbon sink dynamics and supporting the integration of afforestation and forest management strategies into land-use planning (Peng et al., 2025).

Tropical montane forests around the world are undergoing increasing fragmentation, degradation, and deforestation due to human settlement, resource extraction, and land-use change

(Vancutsem et al., 2021). In the central Amazon, nearly 80% of these forests have been lost to expanding agriculture (Bedoya-Garland et al., 2023), resulting in a mosaic landscape of remnant forest patches and intensively managed farmland (Hansen et al., 2020). In Peru, tropical montane forests are located on the eastern slopes of the Andes, between 600 and 3800 masl, accounting for 11.71% of the national territory (Tovar et al., 2010). These forests also play a critical role in safeguarding 97.7% of Peru's water resources, as they are located at the headwaters of the Andean-Amazon basin (Young & León, 2000; Bruijnzeel et al., 2010). This loss of forest cover has significant consequences for ecosystem functioning, including declines in carbon sequestration, soil fertility, and water availability (Noriega-Puglisevich & Eckhardt, 2024).

In recent decades, an increasing number of studies have focused on estimating carbon stored in the aboveground biomass and soils of tropical montane forests (Suhaili et al., 2021; Perea-Ardila et al., 2021; Ramírez et al., 2022; Díaz-Chaux et al., 2023). Despite increasing research on carbon dynamics in tropical ecosystems, substantial gaps remain in our understanding of how carbon stocks respond to gradients of land-use intensification (e.g., Ensslin et al., 2015; Mugagga et al., 2015; De Beenhouwer et al., 2016; van der Sande et al., 2018; Wanyama et al., 2019; Souza et al., 2023). These knowledge gaps are particularly evident in tropical montane forests of Latin America and the Andean region, where studies explicitly assessing the relationship between carbon storage and different land-use types are still limited (Gonzalez et al., 2014). Given the accelerating rates of deforestation and landscape transformation, it is crucial to improve our understanding of how land-use intensification impacts carbon storage in both aboveground biomass and soils, and to identify land-use strategies that can help mitigate carbon loss and preserve biodiversity (Vizcaíno-Bravo et al., 2020).

This study aims to assess variations in aboveground and soil carbon storage along a gradient of land-use intensification, spanning from conserved montane forests to regenerating forests, agroforestry systems, and traditional plantations. Additionally, it evaluates the relationships between vegetation structure, soil physicochemical properties, and carbon storage in both biomass and soil across different land-use types.

2. Methodology

2.1. Study area

The study was conducted in tropical montane forests located on the eastern slope of the Central Andes of Peru, within the province and district of Chanchamayo, in the Junín region. The study area encompasses: (1) the Toro River micro-watershed, and (2) the Pampa Hermosa National Sanctuary (SNPH) (Figure 1).

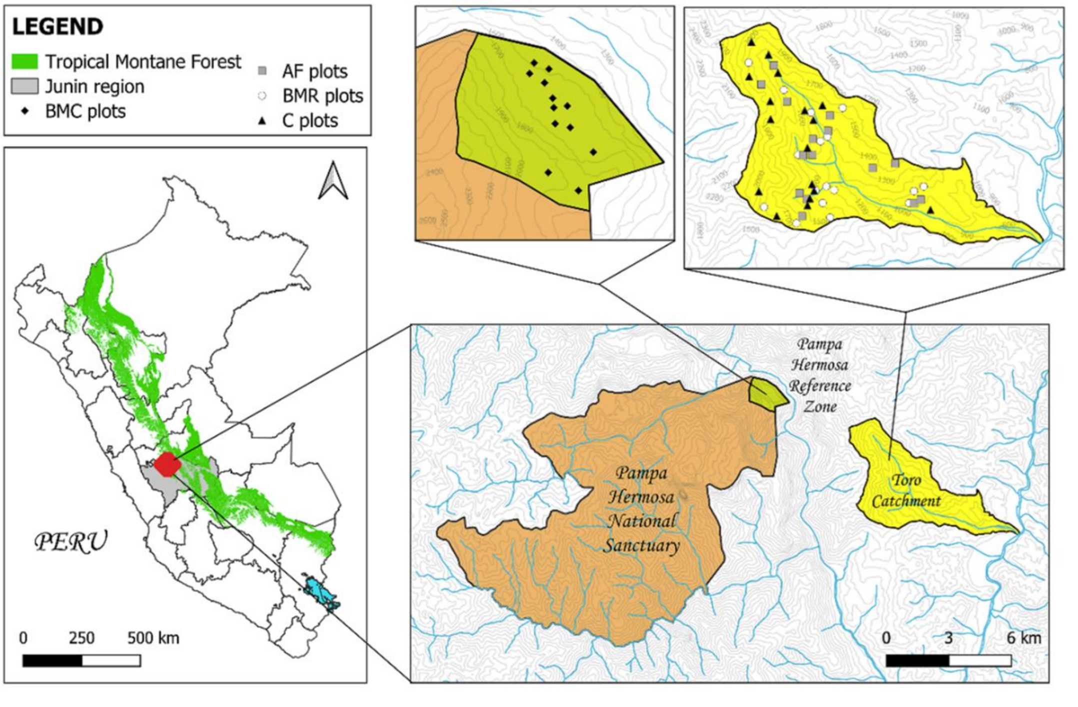

Figure 1. Location of the study area which included: The Pampa Hermosa National Sanctuary and the Toro River micro-watershed, and spatial distribution of sampling plots.

The Toro River sub watershed is located between coordinates 11°0’12.69’’ South latitude and 75° 23’ 37.53’’ West longitude, covering an area of 18.69 km². The terrain is steep, with slopes exceeding 50%, an average annual temperature of 20.9 °C, an annual rainfall of 1623 mm, and an average humidity of 81%. Meteorological data were obtained from the gridded dataset PISCO (Peruvian Interpolation of SENAMHI’s observed climatological and hydrological records). This area has a 250-year history of agricultural, and livestock use, primarily involving coffee monocultures, pastures, and sugarcane. Since the 1980s, coffee has grown with shade species like *Inga feuillei* and *Musa paradisiaca*, alongside the use of mixed fertilizers and herbicides. Livestock and small-scale sugarcane cultivation for aguardiente also persist. A reforestation project initiated 50 years ago introduced species such as *Retrophyllum rospigliosii*, *Piper aduncum*, and *Heliocarpus americanus*.

The conserved montane forests are located within the SNPH, situated on the eastern slope of the Chanchamayo River valley, Junín region, between 11° 3’ 13.46” S latitude and 75° 19’ 9.47” W longitude. The study area within the sanctuary covers 185 hectares, spanning an altitudinal range of 1,200 to 1,700 masl. The SNPH preserves a representative remnant of tropical montane forest, hosting native wildlife and century-old *Cedrela lilloi* trees exceeding 50 m in height (La Torre et al., 2007).

2.2. Classification of Land-Use Types

Land-use classification was developed based on the interpretation of high-resolution Planet satellite imagery (5 m raster format). This interpretation was cross-validated using the Normalized Difference Vegetation Index (NDVI) and ground-truthing through field verification points. Four main land-use types were identified within the study area: (i) Croplands (C), which include areas dedicated to the cultivation of coffee (without shade), maize, rocoto pepper, caigua, passion fruit, and banana, as well as pastures and recently cleared or burned plots; (ii) Agroforestry Systems (AF), characterized by shaded coffee plantations intercropped with banana and avocado, and associated with native or introduced tree species such as *Retrophyllum rospigliosii* (ulcumano), *Juglans neotropica* (Andean walnut), *Inga* spp., *Cedrela odorata* (cedar), and *Ceiba* spp., (iii) Regenerating Montane Forests (BMR), consisting of areas formerly used for agriculture that are undergoing various stages of natural regeneration following abandonment; and (iv) Conserved Montane Forests (BMC), composed of mature forest remnants with minimal anthropogenic disturbance, limited primarily to historical selective logging (Figure 2).

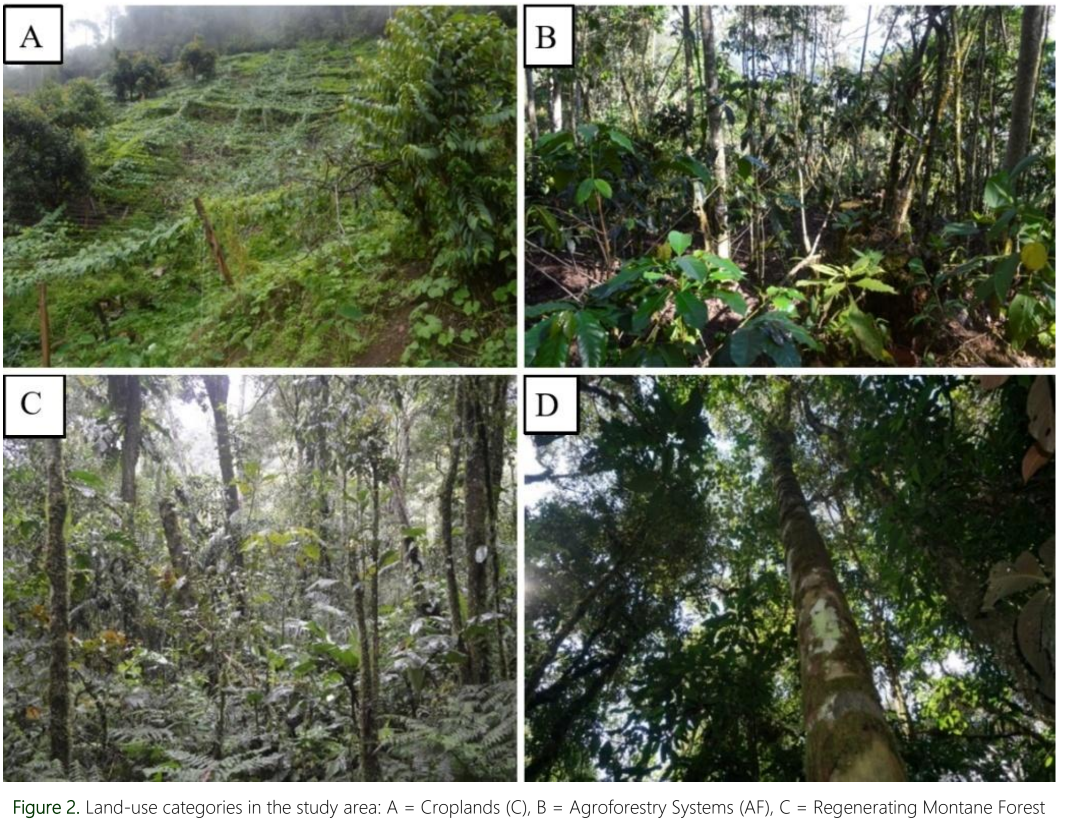

Figure 2. Land-use categories in the study area: A = Croplands (C), B = Agroforestry Systems (AF), C = Regenerating Montane Forest (BMR), and D = Conserved Montane Forest (BMC).

2.3. Methodology

A stratified random sampling design was employed, comprising 61 plots of 0.1 ha each (50 × 20 m), distributed across the four land-use categories: C (n = 17), AF (n = 15), BMR (n = 16), and BMC (n = 13), in accordance with the RAINFOR protocol (Peacock, 2007). Each plot was subdivided into three 10 × 10 m subplots. Within each subplot, data were collected on diameter at breast height (DBH), total tree height, canopy cover, and ground cover by herbaceous vegetation and necromass. Trees were classified into two diameter classes: DC1 (5–30 cm) and DC2 (>30 cm) (Arcanjo et al., 2020).

2.3.1. Soil Organic Carbon (SOC)

In each plot, a soil pit measuring 1 m^3 was excavated, and composite soil samples were collected at five depths (5, 20, 40, 60, and 80 cm). The following parameters were analyzed in the laboratory: organic carbon content (Walkley & Black method), bulk density, pH, electrical conductivity, cation exchange capacity (CEC), organic matter content, soil texture, and macroelements (P, K, Ca, Mg). SOC was calculated based on bulk density, sampling depth, and the percentage of organic carbon in each soil layer. To estimate SOC in MgC ha^{-1}, Equation 1 was used, following the methodology described by Cuellar et al. (2016):

$$SOC = Vs \times C \qquad (1)$$

Where: SOC is the soil organic carbon (MgC ha^{-1}), Vs is the soil volume per hectare (m^3 ha^{-1}), and C is the organic carbon content expressed as a percentage (%).

To assess fine root biomass, soil samples (20 × 20 × 10 cm) were collected down to a depth of 1 m. Fine roots were manually separated, sieved, and dried at 40 °C. Carbon content was estimated based on dry weight, adjusted using a correction factor to account for biomass loss during drying (Cuellar et al., 2015).

2.3.2. Trees and crops

Aboveground biomass was estimated using equations developed for tropical regions with similar climate and precipitation. Specific models were applied for agroforestry trees, considering individuals with DBH ≥ 5 cm and using average wood density from Chave et al. (2005). For coffee plants, diameter (measured 15 cm above ground) and height were recorded for individuals up to 8 cm in diameter (Segura et al., 2006). For banana crops, pseudostem diameter and height were measured for individuals up to 28 cm (Van Noordwijk, 2002) (Table 1).

2.3.3. Necromass and herbaceous vegetation

Dead biomass, comprising standing dead trees, fallen trunks, stumps, and litter, was quantified through direct measurements of diameter and length, with decomposition state (low, medium, and high) considered. Individuals in advanced stages of decomposition were excluded (Noormets et al., 2015). For standing dead trees with branches, live-tree allometric equations were used with a 3% foliage loss adjustment. For trees without branches, stumps, and fallen trunks, a modified volumetric equation was applied using adjusted wood density values (0.38 g/cm^3 for low and 0.22 g/cm^3 for medium decomposition). This method allowed differentiation of necromass carbon by land-use type.

$$B = (0.7854 \times D^2) \times L \times S \quad ...... (2)$$

Where B is dead wood biomass (kg), L is trunk length (cm), D is trunk diameter (cm), and S is wood density (g/cm^3).

In each subplot, three 0.5 × 0.5 m samples of herbaceous plants and litter (dead leaves, dry fruits, and woody debris < 1 cm diameter) were collected and oven-dried at 70 °C to constant weight (Gibbon et al., 2010). The same procedure was used for crop samples (rocoto, corn, granadilla, aromatic herbs, and tubers).

2.6. Data Analysis

The Shapiro-Wilk normality test was applied with a significant level of 5%, with results considered normally distributed when $p \geq 0.05$. A one-way ANOVA was performed, followed by Tukey's test for multiple comparisons between different land uses. When normality assumptions were not met, the non-parametric Kruskal-Wallis test was used, followed by Dunn's post hoc comparisons with Benjamini-Hochberg correction for multiple comparison adjustments. To examine the relationship between environmental variables, Spearman's rank correlation was employed to estimate the correlation between total carbon and soil physical and vegetation structure variables, as well as the relationship between SOC values and physicochemical parameters. To explore and visualize the variability of environmental variables across plots, soil and vegetation variables were analyzed separately using principal component analysis (PCA). Additionally, a multiple comparison test of Principal Components 1 and 2 between land-use types was performed using Tukey's test. Analyses were conducted using PAST v.3.06 and RStudio v.1.4.1106 software.

Table 1
Allometric equations for estimating biomass in multi-species trees and crops

Species/ Crop	Allometric Equations	Autor
General allometric equations	$BA = 0.0509 \times \rho(DBH)^2H$	Chave et al., 2005
Inga sp.	$Log_{10} BA = -0.889 + 2.317 \times log_{10} DBH$	Segura et al. (2006)
Eucalyptus sp.	$BA = 1{,}22 \times DBH^2 \times H \times 0{,}01$	Senelwa y Siens (1998)
Multispecies shade trees	$Log_{10} BA = -0{,}834 + 2{,}223 \times log_{10} DBH$	Segura et al. (2006)
Bambusa sp.	$BA = 0.2223 \times (DBH)^{2.3264}$	Gibbon et al. (2010)
Musa paradisiaca	$BA = 0.030 \times DBH^{2.13}$	Van Noordwijk (2002)
Coffea arabica	$Log_{10} (BA) = -1.113 + 1.578 * Log_{10} (D) + 0.581*Log_{10} (H)$	Segura et al. (2006)

BA: Aboveground biomass (kg); DBH: Diameter at breast height (cm); ρ: Wood density (g/cm^3); H: Total tree height (m).

3. Results and discussion

3.1. Total carbon estimation

The average total carbon values across different land uses show significant differences (KW test H = 23.4, $p < 0.001$) (Table 2). The conserved montane forest (BMC) recorded the highest total carbon storage (575.3 ± 215.4 Mg ha^{-1}), while agricultural lands (C) exhibited the lowest values (205.1 ± 114.0 Mg ha^{-1}), representing a reduction of over 60% in carbon content due to intensified land use. The BMR recorded the second-best average (386.5 ± 186.6 Mg ha^{-1}), followed by AF with an average of 276.7 ± 172.5 Mg ha^{-1}. This difference corresponds to a 28.4% reduction in total carbon storage when transitioning from a regenerating ecosystem to an agroforestry system. Although AF systems do not reach the sequestration potential observed in conserved montane forests, they maintain intermediate storage levels that are significantly higher than those found in conventional agricultural lands.

3.2. Soil Organic Carbon

SOC represents the dominant carbon reservoir across all land uses, contributing between 62% and 93% of the total carbon stock. The highest carbon storage was observed in the BMC (335.3 ± 201.9 Mg ha^{-1}), which significantly surpassed BMR (258.8 ± 151.8 Mg ha^{-1}), AF (194.7 ± 167.6 Mg ha^{-1}), and C (171.4 ± 108.2 Mg ha^{-1}). Differences in SOC across land uses were statistically significant (KW test H = 9.3, $p = 0.026$), suggesting that forest conservation and regeneration contribute to increased carbon accumulation of soil. Although agroforestry systems enhance carbon retention relative to croplands, they do not reach the carbon storage levels observed in forests, primarily due to differences in management practices. The variability in soil carbon content is likely influenced by factors such as organic matter decomposition dynamics, soil compaction, and the accumulation of organic residues. Land use alterations can lead to significant carbon losses from natural and agricultural ecosystems due to erosion, leaching, and enhanced soil respiration (Prakash & Shimrah, 2023).

Fine root carbon was significantly higher in the BMC (36.4 ± 15.4 Mg ha^{-1}) compared to other land uses (KW test H = 24.9, $p < 0.001$). Values dropped sharply in BMR (14.25 ± 7.0 Mg ha^{-1}), AF (12.7 ± 6.6 Mg ha^{-1}), and C (11.9 ± 13.8 Mg ha^{-1}) (Table 2). This result indicates a substantial loss of underground carbon associated with root biomass following forest disturbance, which has direct implications for soil stability, water retention, and nutrient cycling.

Carbon associated with cultivated species was negligible in BMC and BMR, but notable in AF (13.4 ± 6.0 MgC ha^{-1}) and, to a lesser extent, in C (3.2 ± 4.6 MgC ha^{-1}) (Table 2). The higher carbon accumulation in coffee agroforestry systems is explained by the presence of shade trees accompanying the main crop, which enhances carbon capture and storage in both aboveground biomass and soil. These results are consistent with those reported by Ehrenbergerová et al. (2015), who documented that coffee crops grown without shade store less carbon compared to those established in agroforestry systems.

3.3. Aboveground biomass

Aboveground biomass was significantly higher in BMC (187.1 ± 76.5 Mg ha^{-1}), more than double that observed in BMR (100.0 ± 74.3 Mg ha^{-1}), and four times greater than in AF (48.7 ± 24 Mg ha^{-1}) and C (12.5 ± 9.8 Mg ha^{-1}) (KW test H = 45.7, $p < 0.001$) (Table 2). These differences were primarily attributed to the presence of trees with a DBH ≥ 30 cm, which accounted for 51.2% of the total aboveground carbon. In contrast, trees with DBH between 5 and 30 cm, typically associated with regeneration, were more prevalent in BMR (39.5 Mg ha^{-1}), reflecting an active phase of structural recovery.

Aboveground carbon storage in AF systems was 2.4 times higher than in C, due to their more complex vertical structure and presence of shade-tolerant woody species (e.g., *Inga* spp.). These findings confirm that the presence and diversity of woody species in AF systems play a key role in aboveground biomass accumulation and carbon sequestration. However, compared to BMC, AF systems exhibit lower individual density and basal area, which limits their storage potential relative to ecosystems with mature forest structure. The integration of agroforestry systems into productive landscapes significantly enhances carbon stocks compared to monocultures, although it does not reach the levels found in conserved forests (Díaz et al. 2016; Vizcaíno-Bravo et al., 2020).

Herbaceous biomass showed no significant variation across land uses and contributed minimally to total carbon, with an average of 1.0 Mg ha^{-1}. Higher values in C and BMR likely reflect greater light availability. In contrast, necromass, which represented ~4% of total carbon, showed the highest stocks in conserved (BMC: 15.9 ± 8.7 MgC ha^{-1}) and regenerating forests (BMR: 12.1 ± 9.9 MgC ha^{-1}), while significantly lower values were observed in AF (7 ± 4.2 Mg ha^{-1}) and C (4.8 ± 5.5 Mg ha^{-1}) (KW test H = 21.8, p < 0.001) (Figure 3B). The higher accumulation in conserved forests is attributed to the low intensity of anthropogenic disturbance and the continuous input of woody plant material from natural mortality and fall processes (Komposch et al., 2022). In contrast, in agricultural systems, these values are reduced by half, reflecting not only the systematic removal of residues but also the loss of structural complexity in the ecosystem. These results are consistent with those reported for montane tropical forests in Ecuador, where necromass values range from 0.4 to 23 Mg ha^{-1}, with an average of 9.1 Mg ha^{-1} (Wilcke et al., 2005).

Trees with diameters between 5 and 30 cm represent the natural regeneration of the forest and contribute 21% of the total aboveground carbon, with significant variation across land uses (KW test: H = 42.97, p < 0.001) (Figure 3C). The highest carbon content was recorded in BMR (39.5 Mg ha^{-1}), linked to the presence of a new generation of growing trees, which signals an active process of structural recovery. BMC also plays a role in this recovery by hosting mature trees that function as seed producers, with an average carbon content of 30.5 Mg ha^{-1}. In contrast, agricultural systems exhibit lower carbon accumulation, with values of 10.7 Mg ha^{-1} in AF and 2.3 Mg ha^{-1} in C. These findings align with those reported by Ehrenbergerová et al. (2015) for coffee agroforestry systems in the central Amazon of Peru, where carbon content ranged from 27.5 ± 3.2 to 57.5 ± 4.5 Mg ha^{-1}.

Trees with diameters greater than 30 cm show significant differences across land uses (KW test: H = 43.4, p < 0.001) and constitute the primary carbon reservoir, storing 51.2% of the total carbon (Figure 3D). BMC exhibits the highest carbon content in this component, with 140 Mg C ha^{-1}, which is 66% higher than that recorded in BMR, where carbon accumulation reaches 47 Mg C ha^{-1}. In contrast, agricultural systems show significantly lower values, with 17 Mg C ha^{-1} in AF and only 0.75 Mg C ha^{-1} in C. BMC is characterized by well-conserved soils and a high density of mature *Cedrela lilloi* trees, which contribute to substantial carbon storage, both in aboveground biomass and in the soil, due to organic matter accumulation and the presence of large trees that play a key role in long-term carbon capture and sequestration.

3.4. Responses of carbon reserves to environmental and biotic factors

The variations in soil textural fractions (sand, silt, and clay) and bulk density across different land uses are shown in Figure 4. The results reveal differences in soil texture among land-use types, highlighting the influence of management practices and the degree of intervention on soil structure. However, although the values vary across land uses, these differences are not statistically significant, as indicated by the overlapping 95% confidence intervals. BMC presents the best soil quality characteristics, with lower compaction, high organic matter content, elevated CEC, and greater retention of essential cations. In contrast, cropland soils show higher compaction and lower nutrient retention capacity, reflecting the negative impact of intensive agriculture. AF and BMR present an intermediate condition, suggesting that they may be viable strategies for soil quality recovery (Saputra et al., 2020).

Table 2

Total estimated carbon pools in Mg ha^{-1}, with 95% confidence intervals, for the different components by land use in montane forest areas across 0.1 ha plots

Variable (Mg ha^{-1})	BMC Mean	BMC SD	BMR Mean	BMR SD	AF Mean	AF SD	C Mean	C SD	KW test	p value
SOC	335.27 a	201.89	258.78 ab	151.84	194.69 b	167.62	171.35 b	108.20	9.250	0.026
Roots	36.42 a	15.38	14.25 b	6.96	12.47 b	6.46	11.90 b	13.83	24.867	0.000
AGB	187.05 a	76.53	100.02 ab	74.29	48.67 b	24.05	12.46 c	9.79	45.742	0.000
Herbaceous	0.69 ab	0.34	1.34 a	0.97	0.50 b	0.34	1.40 a	1.86	9.914	0.019
Necromass	15.90 a	8.67	12.06 ab	9.94	6.97 bc	4.23	4.81 c	5.49	21.785	0.000
Crop species	0.00 a	0.00	0.08 a	0.31	13.39 b	6.04	3.22 c	4.65	43.427	0.000
Total carbon	575.33 a	215.39	386.53 ab	186.64	276.69 bc	172.52	205.14 c	114.03	23.413	0.000

SD= Standard Deviation; SOC= organic carbon soil; AGB = Aboveground biomass.

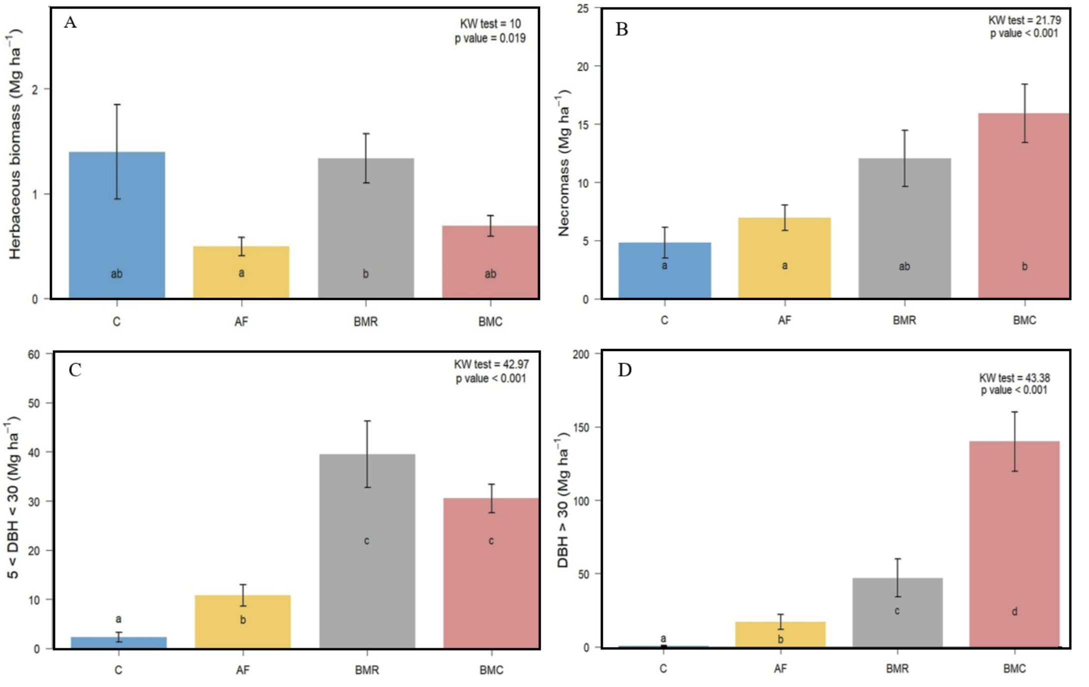

Figure 3. Carbon stock content for (A) herbaceous, (B) necromass, (C) trees with 5–30 cm diameter, and (D) trees with diameters greater than 30 cm (Mg ha^{-1}) across land uses. C=Croplands; AF=Agroforestry Systems; BMR=Regenerating Montane Forest; BMC=Conserved Montane Forest.

The soil texture in BMC is primarily composed of Clay loam (58%) and Clay (25%) (Figure 4). Furthermore, it exhibits low bulk density (g/cm^3), indicating higher water retention capacity and greater porosity, characteristics linked to its high organic matter content (Ruiz et al., 2023). These properties can be attributed to the protective role of the forest canopy, the accumulation of leaf litter, and the stabilization provided by tree roots, which collectively reduce surface soil erosion, enhance porosity, and improve structural stability (Six et al., 2000).

In contrast, soils located in the Toro River subbasin (C, AF, and BMR) exhibit a loam-clay texture (45%) and loam (33%). Sandier textures dominate in AF and BMR, with proportions of 46% and 43%, respectively, which correlates with the higher bulk density recorded ($r = -0.6$, $\rho \approx 1.42$ g/cm^3). Soils with a higher sand content exhibit a reduced capacity for carbon storage, likely due to their limited ability to retain organic matter. This condition is associated with a lower degree of structural aggregation, which restricts water infiltration and aeration, thereby negatively affecting microbial activity and nutrient availability (Soinne et al., 2023).

Land use changes are associated with soil processes and organic carbon content (KW test: $H^2 = 3.224$, $p = 0.073$). The configuration of edaphic properties according to land use type showed distinct spatial patterns, with the first two dimensions of the PCA explaining 55.4% of the total variance (Dim 1: 35.4%; Dim 2: 20.0%) (Figure 5). Dimension 1 represents a gradient associated with soil fertility and water retention capacity, grouping variables such as CEC, wilting point, field capacity, clay content, soil organic carbon, organic matter (O.M.), and exchangeable cations (Ca^{2+}, Mg^{2+}, K^{+}) in the right quadrant. This is supported by positive and significant correlations between SOC and key variables such as O.M. ($\rho = 1.00$, $p < 0.001$), CEC ($\rho \approx 1.00$, $p < 0.001$), Ca^{2+} ($\rho = 0.0060$), cation sum ($p < 0.001$), base sum ($p = 0.0057$), and to a lesser extent, litter ($p = 0.0062$) and bulk density ($p = 0.0236$), although in the latter case, the relationship was inverse (Table A1, Appendix). These correlations indicate that soils with greater physicochemical complexity and structural stability tend to accumulate higher amounts of carbon. This pattern is particularly evident in BMC, which stands out for its high accumulation of organic matter and favorable edaphic structure for carbon storage.

The second dimension of the PCA explained an additional 20% of the variance, distinguishing land uses primarily by complementary textural and physicochemical properties, such as sand content, pH, electrical conductivity, and bulk density. This dimension represented an axis of soil degradation linked to land use practices that cause compaction, loss of structure, and nutrient leaching, conditions common in agricultural lands and some unmanaged agroforestry areas. In this axis, croplands occupied the most degraded end, with elevated Na^+, pH, and bulk density values, alongside low SOC levels. Electrical conductivity exhibited a significant correlation with SOC ($p < 0.001$), highlighting the sensitivity of soil organic carbon to salinity and ionic mobilization. In contrast, slope and altitude, although included in the PCA, showed no significant association with SOC, suggesting that in this Andean context, topographic factors exert less influence than physicochemical soil properties on carbon dynamics.

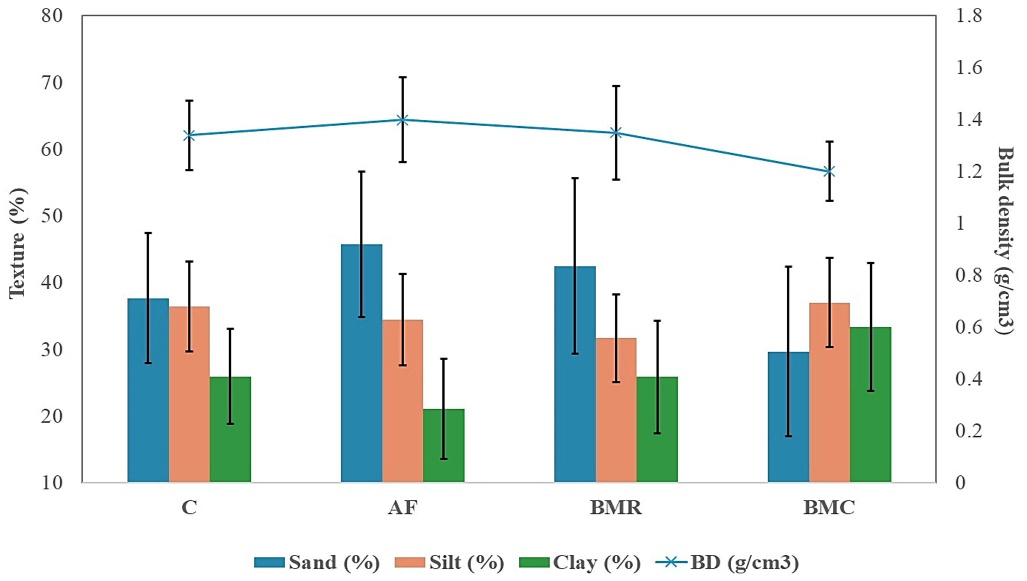

Figure 4. Analysis of soil textural class and bulk density (BD). C=Croplands; AF=Agroforestry Systems; BMR=Regenerating Montane Forest; BMC=Conserved Montane Forest.

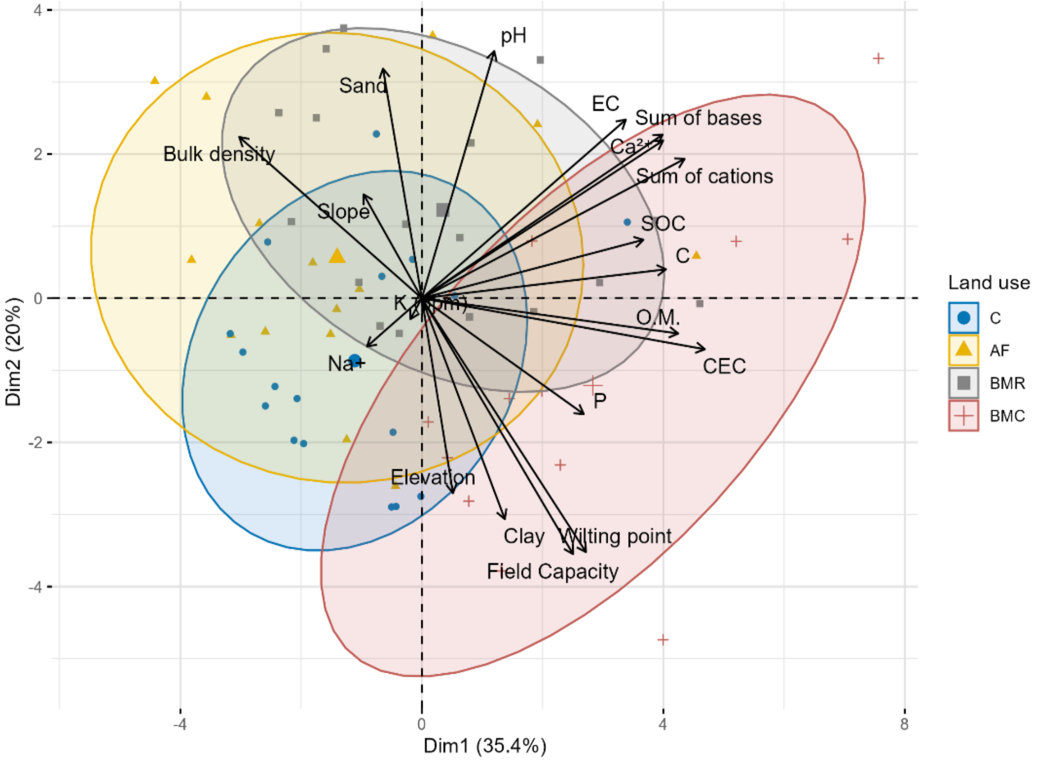

Figure 5. Principal component analysis (PCA) of soil characteristics and land-use types in relation to carbon content variability. OM: Organic Matter; EC: Electrical Conductivity; CEC: Cation Exchange Capacity; SOC: Soil Organic Carbon; P: Phosphorus; Na: Sodium; C: Carbon; K: Potassium. C=Croplands; AF=Agroforestry Systems; BMR=Regenerating Montane Forest; BMC=Conserved Montane Forest.

In contrast, the C and AF land uses were associated with higher sodium (Na^+) concentrations, greater altitudes, steeper slopes, and lower water retention capacity, reflecting processes of soil degradation and quality loss. Dimension 2 (Dim2) represents a combined edaphic and topographic gradient, differentiating soils based on texture, acidity, and drainage capacity. Variables such as sand content, bulk density, and pH are positioned at the upper end of the axis, while phosphorus (P) content, clay, and exchangeable aluminum (Al^{3+}) are grouped at the lower end. This configuration distinguishes between disturbed land uses (C, AF) and those under conservation or recovery (BMC, BMR), indicating differences in water retention, acidity, and edaphic resilience. Disturbed systems exhibit conditions that constrain soil carbon storage, primarily due to reduced structural aggregation and a diminished capacity to stabilize organic matter.

3.5. Aboveground carbon storage and vegetation structure

Different land uses reflect a gradient in biomass and stored carbon, closely linked to vegetation structure. Although the observed differences were not statistically significant (KW test: H = 0.1, p = 0.73; 75% confidence interval), there is a consistent trend suggesting that forest conservation and regeneration promote greater above ground carbon accumulation (Figure 6). The first two dimensions of the PCA jointly explained 39.9% of the total variance (Dimension 1: 27.6%; Dimension 2: 12.3%). Dimension 1 was characterized by the positive grouping of structural variables such as tree biomass (trees with DBH between 5 – 30 cm and >30 cm), basal area, height, and tree density. These patterns are supported by positive and significant correlations between aboveground carbon and tree density in the >30 cm DBH class (DC2) ($\rho = 0.535$, $p = 0.0089$), as well as basal area in DC2 ($\rho = 0.497$, $p = 0.0099$) (Table A2, Appendix). This dimension is interpreted as an axis of structural maturity of the forest ecosystem, with BMC occupying the structurally most developed end, with the highest carbon sequestration capacity, while croplands are grouped at the opposite end, characterized by simplified vegetation structure and low biomass.

Dimension 2 represents an axis of structural transition, where AF exhibited a greater average height among smaller-diameter trees (16.7 m), attributable to the presence of shade species (e.g., *Inga* spp.). Canopy height variability was positively associated with aboveground carbon ($\rho = 0.395$, $p = 0.0088$), suggesting a more vertically complex structure than typically expected in productive systems, characterized by multiple strata and vertical differentiation, features that resemble those of secondary forests (Gusli et al., 2020).

The inverse pattern was observed in conventional agricultural systems, where tree cover is sparse and the area is dominated by herbaceous vegetation with low biomass contribution. The negative correlation between ground cover and aboveground carbon ($\rho = -0.438$, $p = 0.0047$) indicates an inverse relationship between the expansion of non-woody understory species and canopy carbon storage. Necromass and root biomass were also significantly correlated with SOC ($\rho = 0.514$, $p = 0.0150$ and $\rho = 0.296$, $p = 0.0066$, respectively), confirming the role of organic residues and root systems in the dynamics of soil carbon.

Overall, both gradients are closely linked to land-use changes. Forest conservation occupies the most favorable extremes of both axes, exhibiting the highest carbon stocks in both soil and biomass. In contrast, intensive agricultural systems are located at the opposite ends, characterized by degraded soils and simplified vegetation structures, with losses of up to 60% of total carbon. Intermediate systems (BMR and AF) display potential for ecological recovery, particularly when management practices enhance soil structure and incorporate functional woody species.

Vegetation is a key driver of both the quantity and quality of soil organic matter, primarily through the input of plant residues that differ in decomposition rates and nutrient composition (Sun, 2024). Climatic factors, particularly temperature and precipitation, regulate the decomposition and stabilization of organic matter, favoring carbon sequestration in temperate and humid environments (Huang et al., 2024). Topographic features, such as slope, can also influence carbon dynamics by promoting organic matter accumulation in valley-bottom soils (Zhou, 2023). Within this framework, intensive agricultural practices often exacerbate carbon losses, underscoring the importance of adopting sustainable land-use strategies, such as agroforestry systems, that enhance soil resilience and carbon retention (Pan et al., 2024). These findings are supported by studies indicating that agroforestry and regenerating systems have high potential for enhancing soil carbon sequestration and contributing to climate change mitigation (Pan et al., 2024; Montagnini, 2004). Moreover, such systems promote biodiversity, improve soil structure and fertility, and reduce erosion, while also providing sustainable economic benefits through diversified crop production and timber yields (Crespo et al., 2023; VijayKumar et al., 2024).

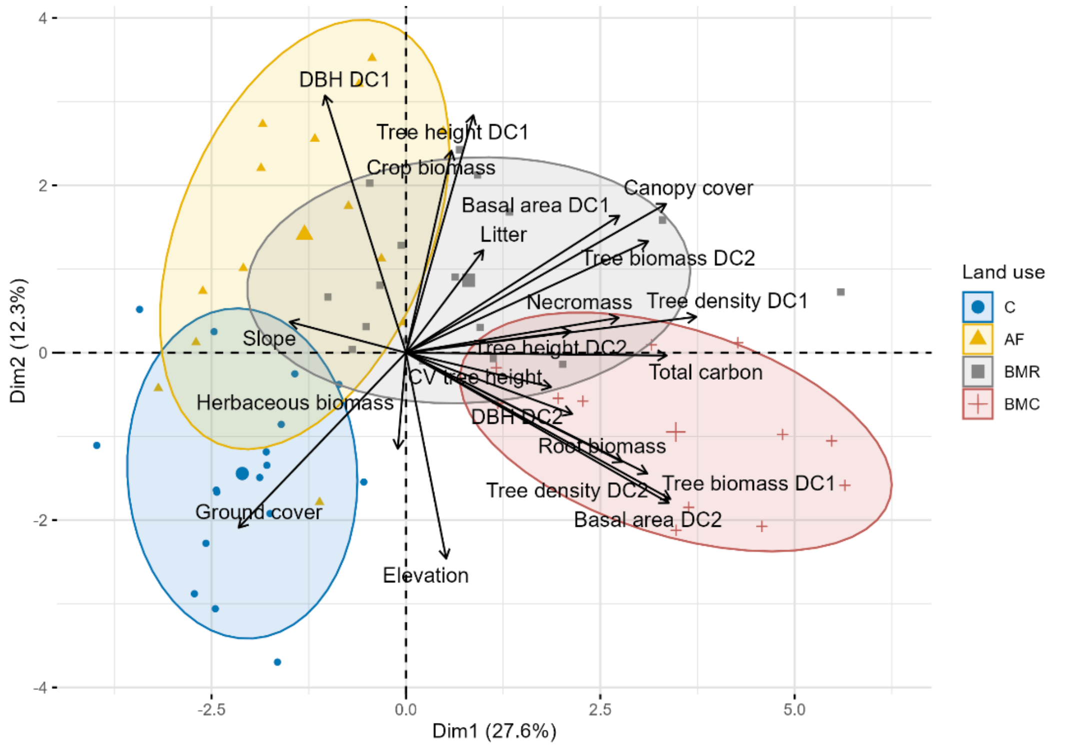

Figure 6. Principal component analysis (PCA) of vegetation structural attributes and land-use types in relation to carbon content variability. The direction and length of the vectors indicate the effect of each variable.
OM: Organic Matter; EC: Electrical Conductivity; CEC: Cation Exchange Capacity; SOC: Soil Organic Carbon; P: Phosphorus; Na: Sodium; C: Carbon; K: Potassium.
C=Croplands; AF=Agroforestry Systems; BMR=Regenerating Montane Forest; BMC=Conserved Montane Forest.

4. Conclusions

This study demonstrates that carbon storage in tropical montane landscapes of the Central Andes of Peru is strongly influenced by land use, which in turn shapes both vegetation structure and soil properties. Less-disturbed forests exhibited the highest levels of SOC and aboveground carbon, in stark contrast to areas under agricultural use. This variability is driven by multiple factors, including changes in vegetation cover, agricultural practices, and climatic conditions.

Restoring degraded areas could lead to a recovery of approximately 25% of SOC when transitioning from BMR to BMC, with a further 14% increase observed when trees are incorporated into monoculture systems. These findings underscore the potential of agroforestry systems to enhance SOC content. Moreover, the results confirm that SOC constitutes the principal carbon reservoir in tropical montane forests, irrespective of land use. Trees with a DBH ≥ 30 cm emerge as reliable indicators of conserved forests, while those with a DBH between 5 and 30 cm are indicative of regenerating forest stands. The results suggest that management practices focused on conserving forest cover and improving soil properties can maximize ecosystem services related to carbon storage. These findings underscore the need to integrate soil management and the restoration of vegetation structure as complementary strategies for climate change mitigation in mountain ecosystems.

Active restoration of degraded forests and the expansion of diverse agroforestry systems offer valuable opportunities to reverse carbon losses, restore ecosystem functions, and enhance the resilience of tropical agricultural landscapes. Conserving and restoring forest structure and soil functionality is essential to reinforce the role of Andean landscapes as carbon sinks. This integrated approach is crucial for informing climate mitigation policies and sustainable land management, and it emphasizes the importance of considering synergies between aboveground and soil carbon in the planning of REDD+ initiatives, resilient agroforestry systems, and ecological restoration strategies.

While this study highlights important variations across the gradients of land-use intensification, future research could also emphasize long-term monitoring of aboveground and soil carbon to track recovery in regenerating forests and agroforestry systems. Incorporating greenhouse gas fluxes (CO_2, CH_4, N_2O) would further complement stock estimates by capturing the dynamics of carbon and ecosystem processes. Additionally, understanding the socioeconomic drivers and consequences of adopting regenerative forests and agroforestry systems is essential for promoting more sustainable practices in the region. Comparative studies across the Andes are particularly needed to identify the most successful practices, providing elements for a cost-benefit analysis that consider both the long-term capacity of montane landscapes to function as carbon sinks and their ability to adapt to the impacts of climate change on agricultural practices.

Acknowledgments

This study was funded by Universidad Científica del Sur as part of the "Fondo Semilla 2019-2" Research Projects Contest for Faculty. We express our sincere gratitude to the farmers of the Toro sub-basin for granting access to their lands during the sampling phase and for their hospitality throughout the study, particularly the Gerbi and Ñaupa families. We also extend our thanks to Violeta Valderrama, Fausto Corsino, Carlo Mario Orihuela, and Adaia Alegre for their invaluable assistance in vegetation and soil sampling, as well as to the students from the Faculty of Environmental Sciences at Universidad Científica del Sur for their support during the fieldwork. We thank Jorge Ruiz for his support with the statistical analyses and the preparation of the figures.

Author contributions

K. I. Eckhardt: conceptualization, methodology, writing original draft, formal analysis, results interpretation and discussion. A. G. Maia: review and editing, validation, formal analysis and methodological supervision; J. A. Noriega-Puglisevich: data collection, data curation, laboratory analysis (soil carbon), review and editing.; W. Cachay Jara: data collection, data curation and discussion of results (aboveground carbon).

ORCID

K. I. Eckhardt https://orcid.org/0000-0001-6165-6597
A. G. Maia https://orcid.org/0000-0003-0075-5094
J. A. Noriega-Puglisevich https://orcid.org/0000-0003-4510-7314
W. Cachay Jara https://orcid.org/0000-0002-2165-1190

References

Arcanjo, F. A., Taglianetti, E., & Torezan, J. M. D. (2020). Big trees, big fall: Large-diameter trees and the fate of carbon stocks in Atlantic Forest remnants. *Oecologia Australis*, *24*(2), 438–447. https://doi.org/10.4257/oeco.2020.2402.14

Bedoya-Garland, E., Aramburú, C. E., & López-de-Romaña, A. (2023). La producción de nuevas naturalezas en la alta Amazonía peruana (1940–1981) y las tesis de Ester Boserup. *Revista Kawsaypacha: Sociedad y Medio Ambiente*, *12*, A-008. https://doi.org/10.18800/kawsaypacha.202302.A008

Bruijnzeel, L. A., Mulligan, M., & Scatena, F. N. (2010). Hydrometeorology of tropical montane cloud forests: Emerging patterns. *Hydrological Processes*, *24*(3), 385–398. https://doi.org/10.1002/hyp.7974

Chave, J., Andalo, C., Brown, S., Cairns, M. A., Chambers, J. Q., Eamus, D., Fölster, H., Fromard, F., Higuchi, N., Kira, T., Lescure, J. P., Nelson, B. W., Ogawa, H., Puig, H., Riéra, B., & Yamakura, T. (2005). Tree allometry and improved estimation of carbon stocks and balance in tropical forests. *Oecologia*, *145*, 87–99. https://doi.org/10.1007/s00442-005-0100-x

Cuellar Bautista, J. E., & Salazar Hinostroza, E. J. (2016). *Dinámica del carbono almacenado en los diferentes sistemas de uso de la tierra en el Perú.* Instituto Nacional de Innovación Agraria (INIA). https://repositorio.inia.gob.pe/handle/20.500.12955/490

Cuellar, J., Salazar, E., & Fernández, K. (2015). Efecto del cambio de uso del bosque tropical sobre carbono total almacenado, cuenca de Aguaytía, Perú. *Revista Forestal del Perú*, *27*(1–2), 7–25. https://repositorio.inia.gob.pe/handle/20.500.12955/559

Crespo, A. M., Souza, M. N., & Silva, M. A. B. da. (2023). Ciclo do carbono e sistemas agroflorestais na sustentabilidade da produção agrícola: Revisão de literatura. *Incaper em Revista*, *13–14*, 6–19. https://doi.org/10.54682/ier.v.13e14.p06.19

De Beenhouwer, M., Geeraert, L., Mertens, J., Van Geel, M., Aerts, R., Vanderhaegen, K., & Honnay, O. (2016). Biodiversity and carbon storage co-benefits of coffee agroforestry across a gradient of increasing management intensity in the SW Ethiopian highlands. *Agriculture, Ecosystems & Environment*, *222*, 193–199. https://doi.org/10.1016/j.agee.2016.02.017

Debie, R., & Abro, T. W. (2025). Carbon stock dynamics in biosphere reserves and mountainous forest ecosystems. *Trees, Forests and People*, *19*, 100789. https://doi.org/10.1016/j.tfp.2025.100789

Díaz, P., Fachin, G., Tello, C., & Arévalo, L. (2016). Carbono almacenado en cinco sistemas de uso de tierra en la región San Martín, Perú. *Revista Internacional de Desarrollo Regional Sustentable*, *1*(2), 57–67.

Díaz-Cháux, J. T., Ordoñez-García, M. A., Cerón, C. T., & Velázquez-Valencia, A. (2024). Biomasa y carbono almacenado en bosques de la Amazonia colombiana. *Caldasia*, *46*(1). https://doi.org/10.15446/caldasia.v46n1.99728

Ehrenbergerová, L., Cienciala, E., Kučera, A., Guy, L., & Habrová, H. (2015). Carbon stock in agroforestry coffee plantations with different shade trees in Villa Rica, Peru. *Agroforestry Systems*, *90*, 433–445. https://doi.org/10.1007/s10457-015-9865-z

Ensslin, A., Rutten, G., Pommer, U., Zimmermann, R., Hemp, A., & Fischer, M. (2015). Effects of elevation and land use on the biomass of trees, shrubs and herbs at Mount Kilimanjaro. *Ecosphere*, *6*(3), 1–15. https://doi.org/10.1890/es14-00492.1

Gibbon, A., Silman, M., Malhi, Y., Fisher, J., Meir, P., Zimmermann, M., Dargie, G., Farfan, W., & Garcia, K. (2010). Ecosystem carbon storage across the grassland–forest transition in the high Andes of Manu National Park, Peru. *Ecosystems*, *13*(7), 1097–1111. https://doi.org/10.1007/s10021-010-9376-8

Gonzalez, R., Kroll, L., & Vargas, R. (2014). Carbon stocks and dynamics in Andean montane forests: Linking soil and vegetation under land-use change scenarios. *Journal of Environmental Management*, *143*, 95–104. https://doi.org/10.1016/j.jenvman.2014.04.006

Gusli, S., Sumeni, S., Sabodin, R., Muqfi, I. H., Nur, M., Hairiah, K., Useng, D., & Van Noordwijk, M. (2020). Soil organic matter, mitigation of and adaptation to climate change in cocoa-based agroforestry systems. *Land*, *9*(9), 323. https://doi.org/10.3390/land9090323

Hansen, M. C., Wang, L., Song, X. P., Tyukavina, A., Turubanova, S., Potapov, P. V., & Stehman, S. V. (2020). The fate of tropical forest fragments. *Science Advances*, *6*(11), eaax8574. https://doi.org/10.1126/sciadv.aax8574

Huang, X., Ibrahim, M. M., Luo, Y., Jiang, L., Chen, J., & Hou, E. (2024). Land-use change alters soil organic carbon: Constrained global patterns and predictors. *Earth's Future*, *12*(5). https://doi.org/10.1029/2023EF00425

Komposch, A., Ensslin, A., Fischer, M., & Hemp, A. (2022). Aboveground deadwood biomass and composition along elevation and land-use gradients at Mount Kilimanjaro. *Frontiers in Ecology and Evolution*, *9*, 732092. https://doi.org/10.3389/fevo.2021.732092

La Torre, M., Herrando, S., & Young, K. (2007). Diversity and structural patterns for tropical montane and premontane forests of central Peru, with an assessment of the use of higher-taxon surrogacy. *Biodiversity and Conservation*, *16*(10), 2965–2988. https://doi.org/10.1007/s10531-007-9155-9

Noriega-Puglisevich, J. A., & Eckhardt, K. I. (2024). Hydrological effects of the conversion of tropical montane forests to agricultural land in the central Andes of Peru. *Environmental Quality Management*, 1–11. https://doi.org/10.1002/tqem.22221

Montagnini, F., & Nair, P. (2004). Carbon sequestration: An underexploited environmental benefit of agroforestry systems. *Agroforestry Systems*, *61–62*(1–3), 281–295. https://doi.org/10.1023/B:AGFO.0000029005.92691.79

Mugagga, F., Buyinza, M., Nabanoga, G. N., & Katongole, C. (2015). Land use change, policy, and forest transitions in Uganda: A century of forest loss and recovery. *Forest Policy and Economics*, *50*, 1–9. https://doi.org/10.1016/j.forpol.2014.06.005

Noormets, A., Epron, D., Domec, J., McNulty, S., Fox, T., Sun, G., & King, J. (2015). Effects of forest management on productivity and carbon sequestration: A review and hypothesis. *Forest Ecology and Management*, *355*, 124–140. https://doi.org/10.1016/j.foreco.2015.05.019

Ojoatre, S., Barlow, J., Jacobs, S. R., & Rufino, M. C. (2024). Recovery of aboveground biomass, soil carbon stocks and species diversity in tropical montane secondary forests of East Africa. *Forest Ecology and Management*, *552*, 121569. https://doi.org/10.1016/j.foreco.2023.121569

Pan, J., Chen, S., He, D., Zhou, H., Ning, K., Ma, N., Li, K., Liao, D., Mi, W., Wu, Q., Zhang, C., & Dong, Z. (2024). Agroforestry increases soil carbon sequestration, especially in arid areas: A global meta-analysis. *Catena*, *249*, 108667. https://doi.org/10.1016/j.catena.2024.108667

Peacock, J., Baker, T. R., Lewis, S. L., López-González, G., & Phillips, O. L. (2007). The RAINFOR database: Monitoring forest biomass and dynamics. *Journal of Vegetation Science*, *18*(4), 535–542. http://www.jstor.org/stable/4499259

Peng, D., Zhang, B., Zheng, S., et al. (2025). Newly established forests dominated global carbon sequestration change induced by land cover conversions. *Nature Communications*, *16*, 6570. https://doi.org/10.1038/s41467-025-61956-y

Perea-Ardila, M. A., Andrade-Castañeda, H. J., & Segura-Madrigal, M. A. (2021). Estimación de biomasa aérea y carbono con teledetección en bosques altoandinos de Boyacá, Colombia: Estudio de caso Santuario de Fauna y Flora Iguaque. *Revista Cartográfica*, *102*, 91–123. https://doi.org/10.35424/rcarto.i102.821

Prada, C. M., Heineman, K. D., Pardo, M. J., Piponiot, C., & Dalling, J. W. (2025). Soil and biomass carbon storage is much higher in Central American than Andean montane forests. *Biogeosciences*, *22*, 3615–3634. https://doi.org/10.5194/bg-22-3615-2025

Prakash, T., & Shimrah, T. (2023). A review on soil carbon sequestration in different land use and land cover. *Ecology, Environment and Conservation, 29*(Suppl. Issue 3), S332–S340. https://doi.org/10.53550/EEC.2023.v29i03s.060

Ramírez, J., Córdova, M., Imbaquingo, J., & Chagna, E. (2022). Modelos alométricos para estimar biomasa aérea en bosques secundarios montanos del noroccidente de Ecuador. *Caldasia*, *44*(1), 82–94. https://doi.org/10.15446/caldasia.v44n1.88198

Ruiz, A., Ruiz-Sagaseta, A., Orcaray, L., Arricibita, F. J., Enrique, A., Soto, I. D., & Virto, I. (2021). Soil water retention and soil compaction assessment in a regional-scale strategy to improve climate change adaptation of agriculture in Navarre, Spain. *Agronomy*, *11*(3), 607. https://doi.org/10.3390/agronomy11030607

Saputra, D., Sari, R., Hairiah, K., Roshetko, J., Suprayogo, D., & van Noordwijk, M. (2020). Can cocoa agroforestry restore degraded soil structure? *Agroforestry Systems*, *94*, 2261–2276. https://doi.org/10.1007/s10457-020-00548-9

Segura, M., Kanninen, M., & Suárez, D. (2006). Allometric models for estimating aboveground biomass of shade trees and coffee bushes grown together. *Agroforestry Systems*, *68*(2), 143–150. https://doi.org/10.1007/s10457-006-9005-x

Senelwa, K., & Sims, R. E. H. (1998). Tree biomass equations for short rotation eucalypts grown in New Zealand. *Biomass and Bioenergy*, *13*(3), 133–140. https://doi.org/10.1016/S0961-9534(97)00026-3

Six, J., Paustian, K., Elliott, E. T., & Combrink, C. (2000). Soil structure and organic matter: I. Distribution of aggregate-size classes and aggregate-associated carbon. *Soil Science Society of America Journal*, *64*(2), 681–689. https://doi.org/10.2136/sssaj2000.642681x

Soinne, H., Keskinen, R., Tähtikarhu, M., Kuva, J., & Hyväluoma, J. (2023). Effects of organic carbon and clay contents on structure-related properties of arable soils with high clay content. *European Journal of Soil Science*, *74*(5), e13424. https://doi.org/10.1111/ejss.13424

Suhaili, N. S., Mhd Hatta, S., James, D., Hassan, A., Jalloh, M. B., Phua, M.-H., & Awang Besar, N. (2021). Soil carbon stocks and litterfall fluxes from the Bornean tropical montane forests, Sabah, Malaysia. *Forests*, *12*(12), 1621. https://doi.org/10.3390/f12121621

Sun, Y., Wang, X., Zhang, Y., Duan, W., Xia, J., Wu, J., & Deng, T. (2024). Vegetation types can affect soil organic carbon and $\delta^{13}C$ by influencing plant inputs in topsoil and microbial residue carbon composition in subsoil. *Sustainability*, *16*(11), 4538. https://doi.org/10.3390/su16114538

Tovar, A., Tovar, C., Saito, J., Soto, A., Regal, F., Cruz, Z., Véliz, C., Vásquez, P., & Rivera, G. (2010). *Yungas peruanas – Montane forests of the eastern slope of the Andes of Peru: An ecoregional perspective of conservation*. Data Center for Conservation, Faculty of Forestry, National Agrarian University La Molina.

van Noordwijk, M., Rahayu, S., Hairiah, K., Wulan, Y. C., Farida, A., & Verbist, B. (2002). Carbon stock assessment for a forest-to-coffee conversion landscape in Sumber-Jaya (Lampung, Indonesia): From allometric equations to land use change analysis. *Science in China Series C: Life Sciences*, *45*(Suppl.), 75–86.

van der Sande, M. T., Arets, E. J., Peña-Claros, M., Hoosbeek, M. R., Cáceres-Siani, Y., van der Hout, P., & Poorter, L. (2018). Soil fertility and species traits, but not diversity, drive productivity and biomass stocks in a Guyanese tropical rainforest. *Functional Ecology*, *32*(2), 461–474. https://doi.org/10.1111/1365-2435.12968

Vancutsem, C., Achard, F., Pekel, J.-F., Vieilledent, G., Carboni, S., Simonetti, D., Gallego, J., Aragão, L. E. O. C., & Nasi, R. (2021). Long-term (1990–2019) monitoring of forest cover changes in the humid tropics. *Science Advances*, *7*(10), eabe1603. https://doi.org/10.1126/sciadv.abe1603

VijayKumar, R., Tiwari, P., Daniel, S., Kumar, K. R., Mishra, I., Aneesh, K. S., & Shah, D. (2024). Agroforestry systems: A pathway to resilient and productive landscapes. *International Journal of Environment and Climate Change*, *14*(12), 177–193. https://doi.org/10.9734/ijecc/2024/v14i124617

Vizcaíno-Bravo, Q., Williams-Linera, G., & Asbjornsen, H. (2020). Biodiversity and carbon storage are correlated along a land use intensity gradient in a tropical montane forest watershed, Mexico. *Basic and Applied Ecology*, *44*, 24–34. https://doi.org/10.1016/j.baae.2019.12.004

Wanyama, I., Pelster, D. E., Butterbach-Bahl, K., Verchot, L. V., Martius, C., & Rufino, M. C. (2019). Soil carbon dioxide and methane fluxes from forests and other land use types in an African tropical montane region. *Biogeochemistry*, *143*(2), 171–190. https://doi.org/10.1007/s10533-019-00555-8

Wilcke, W., Hess, T., Bengel, C., Homeier, J., Valarezo, C., & Zech, W. (2005). Coarse woody debris in a montane forest in Ecuador: Mass, C and nutrient stock, and turnover. *Forest Ecology and Management*, *205*(1–3), 139–147. https://doi.org/10.1016/j.foreco.2004.10.044

Young, K., & León, B. (2000). Biodiversity conservation in Peru's eastern montane forests. *Mountain Research and Development*, *20*(3), 208–211. https://doi.org/10.1659/0276-4741(2000)020

Zhou, T., Lv, Y., Xie, B., Xu, L., Zhou, Y., Mei, T., Li, Y., Yuan, N., & Shi, Y. (2023). Topography and soil organic carbon in subtropical forests of China. *Forests*, *14*(5), 1023. https://doi.org/10.3390/f14051023

Appendix 1

Spearman correlations between vegetation structural, edaphic, and carbon-related variables

Table A1

Spearman correlation between edaphic variables and SOC

Independent variable	ρ with Soil Organic Carbon (SOC)	p value	Significance
Elevation	0.1729	0.1826	ns
Slope	0.0554	0.6717	ns
pH	0.0848	0.5159	ns
EC	0.4513	0.0003	**
C	0.9581	< 0.0001	***
P	0.3468	0.0062	**
K (ppm)	-0.259	0.0435	*
Sand	0.186	0.1512	ns
Clay	-0.091	0.4839	ns
CEC	0.6135	1.4641E-07	***
Ca^{2+}	0.3478	0.0060	**
Na^{+}	-0.207	0.1098	ns
Sum of cations	0.477	0.0001	***
Sum of bases	0.3502	0.0057	**
Bulk density	-0.2895	0.0236	*
Wilting point	0.3598	0.0044	**
O.M.	0.8261	2.4956E-16	***
Field capacity	0.3172	0.0127	*

*p < 0.05, **p < 0.01, ***p < 0.001, ns = not significant (p ≥ 0.05).

Table A2

Spearman Correlation Coefficients (ρ) between Total Aboveground Carbon and Vegetation Structural Variables

Independent Variable	ρ with Total Carbon stock	p value	Significance
Canopy cover	0.581	0.0012	***
Tree density DC2	0.535	0.0089	**
Basal area DC2	0.497	0.0099	**
Tree biomass DC1	0.563	0.0048	**
Tree biomass DC2	0.456	0.0870	n.s.
Basal area DC1	0.285	0.3120	n.s.
Tree density DC1	0.558	0.0991	n.s.
DBH DC2	0.254	0.0490	*
DBH DC1	-0.194	0.1460	n.s.
Tree height DC1	0.145	0.1600	n.s.
Tree height DC2	0.160	0.1600	n.s.
CV tree height	0.395	0.0088	**
Slope	-0.081	0.7300	n.s.
Elevation	0.119	0.6200	n.s.
Ground cover	-0.438	0.0047	**
Litter	0.363	0.0012	***
Herbaceous biomass	0.025	1.0000	n.s.
Necromass	0.514	0.0150	*
Root biomass	0.296	0.0066	**
Crop biomass	0.183	1.0000	n.s.

DC1: Trees with DBH of 5–30 cm
DC2: Trees with DBH >30 cm
n.s.: not significant
*p < 0.001, p < 0.01, p < 0.05